Research Article Vol. 59, No. 28 / 1 October 2020 / Applied Optics 8789

High-order DBR semiconductor lasers: effect of grating parameters on grating performance

Siyu E,[1,2] Yinli Zhou,[1,*] Xing Zhang,[1] Jianwei Zhang,[1] Youwen Huang,[1] Yugang Zeng,[1] Jinjiang Cui,[3,4] Yun Liu,[1] Yongqiang Ning,[1] and Lijun Wang[1]

[1]State Key Laboratory of Luminescence and Applications, Changchun Institute of Optics, Fine Mechanics and Physics, Changchun 130033, China
[2]University of Chinese Academy of Sciences, Beijing 100049, China
[3]Suzhou Institute of Biomedical Engineering and Technology, Chinese Academy of Sciences, Suzhou 215163, China
[4]Jinan Guoke Medical Science and Technology Development Co., Ltd., Jinan 250000, China
*Corresponding author: zhouyinli@ciomp.ac.cn

Received 14 July 2020; revised 26 August 2020; accepted 5 September 2020; posted 9 September 2020 (Doc. ID 402699); published 28 September 2020

In this paper, a high-order distributed Bragg reflector (DBR) semiconductor laser operating at 1064 nm is demonstrated based on simulation analysis. To get optimal Bragg grating characteristics, four parameters of the Bragg grating were analyzed in detail. Forty-nine-order Bragg gratings were designed with a reflectivity of 6% and a FWHM of 3 nm, which can realize mode selection while lasing. The Bragg gratings were designed to maximize the use of light. Transmission of the rear laser facet is theoretically 0. This simulation result provides a simple and efficient DBR semiconductor laser scheme without cavity surface coating.

https://doi.org/10.1364/AO.402699

1. INTRODUCTION

Narrow-linewidth semiconductor lasers are widely used in space laser communication [1], precision measurement [2], and pumping solid-state lasers and fiber lasers [3] for their excellent spectral and coherent characteristics.

The techniques used to achieve narrow-linewidth lasers can be broadly divided into two categories. One approach is to use a mode-selection device outside the laser cavity to control gain and loss at different wavelengths [4,5]. External cavity lasers (ECLs) that use a diffraction grating as the feedback element usually use the Littrow or Littman structure [6]. By adopting a side-of-fringe stabilization technology to achieve active frequency stabilization, an ECL with a wavelength tuning range of 60 nm and a linewidth of 160 kHz was achieved [7], and the linewidth is narrowed down to 400 Hz later by the same research team [8]. Another way is integrating a frequency-selective structure [distributed feedback (DFB) or distributed Bragg reflector (DBR)] in a resonant cavity [9,10]. The DFB laser usually distributes the Bragg grating structure in the entire resonant cavity, which mainly plays the role of optical feedback mode selection and gain [11]. The DBR laser has a very strong reflection effect on the optical mode that meets the Bragg conditions [12–14]. Decker *et al.* [15] fabricate high-order DFB grating on a narrow stripe broad area laser, and the device achieved a power of 6 W and a laser linewidth of 130.7 GHz. The external cavity techniques for narrow-linewidth lasers require complex and large-scale optical devices. And most of the inner cavity techniques require a cavity surface coating process or a curved waveguide to avoid the influence of the reflected light from the rear cavity surface on the laser frequency characteristics.

For DBR semiconductor lasers, the change of grating parameters will directly affect the performance of the grating. Under the same conditions as duty cycle, etching depth, grating length, and grating material, the reflectivity of the grating decreases as the order of the grating increases. Therefore, the reflectivity of high-order gratings is relatively low compared to other grating structures. However, the fabrication process of the high-order gratings is much simpler, and the lithography limit demand of the lithography machine is only 1 μm. In contrast, the fabrication precision required for low-order gratings is generally a few hundred nanometers or even lower, requiring a more complicated fabrication process, such as electron beam lithography [16] or laser holographic lithography. In this paper, we designed a 49-order DBR semiconductor laser operating at 1064 nm that can make the best use of light without cavity surface coating. By particularly analyzing the effects of grating parameters on the spectral performance of the laser, a set of suitable grating structure parameters is obtained leading to zero transmission at the rear cavity surface of the laser.

2. EPITAXIAL STRUCTURE AND GRATING PARAMETERS

The sketch of the epitaxial structure and grating structure is shown in Fig. 1(a). A symmetrical waveguide layer of 1.2 μm

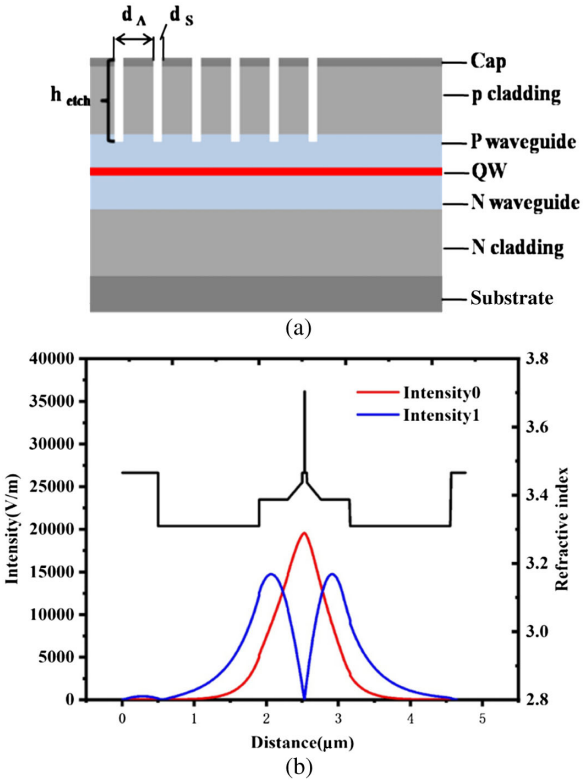

Fig. 1. (a) Schematic diagram of the epitaxial and grating structure. (b) Electric field intensity distribution and refractive index distribution along the epitaxial direction.

thickness is adopted, and a 20 nm quantum well (QW) layer with a lasing wavelength of 1064 nm is inserted in the middle of the waveguide layer (Table 1). The P cladding and N cladding layers are both 1.4 μm. The main grating parameters being researched include the grating period d_Λ, slot width d_s, etching depth h_{etch}, and number of gratings N. The electric field distribution and refractive index distribution of the epitaxial structure are shown in Fig. 1(b). The peak of the fundamental mode is mainly concentrated near the quantum well layer. The ratio of the fundamental mode to the higher-order mode optical limiting factors is 5580, which can keep the laser operating at a stable single fundamental mode.

Table 1. Specific Data of Epitaxial Structure

Layer Name	Material Type	Composition of Al or In	Thickness (nm)
Cap	GaAs	0%	200
P cladding	AlGaAs	33%	1400
P waveguide	AlGaAs	20%	400
P confinement	AlGaAs	5%∼20%	200
Barrier	GaAs	0%	30
Quantum well	InGaAs	22%	5
Barrier	GaAs	0%	30
N confinement	AlGaAs	5%∼20%	200
N waveguide	AlGaAs	20%	400
N cladding	AlGaAs	33%	1400
Substrate	GaAs	0%	500

The simulation methods for DBR gratings are mainly the following: the one-dimensional transfer matrix method [17], the two-dimensional scattering matrix method (SMM) [18], the approximate coupled-mode theory [19], the finite-difference time-domain method [20], etc. This paper combines the SMM and the finite element method to simulate the performance of the DBR grating. The influence of the parameters of one grating on the spectral characteristics of the DBR laser was investigated by the finite element method using COMSOL software. Then, the SMM was used to calculate the characteristics of multiple pairs of gratings. The number of gratings N was initially set to 200 to ensure maximum utilization of the light in the gratings. The influence of the number of gratings N on the spectrum characteristics was studied in the end.

3. RESULTS AND DISCUSSION

First, the effect of grating period d_Λ on the spectral features was analyzed. The slot width d_s and the etching depth h_{etch} were fixed to 1500 nm and 1650 nm, respectively. The reflectivity of 200 pairs of gratings versus different d_Λ is shown in Fig. 2. A set of peak reflectivity values appears with a period of 157 nm and is almost uniform, which indicates that the grating period does not affect the maximum reflectivity of the grating. To further study the effect of the grating period on the full width at half maximum (FWHM) of the reflectivity curve, we have selected five of the grating periods obtained above (the top five reflectivity values). The five selected grating periods are 3450 nm, 5487 nm, 7681 nm, 9875 nm, and 11912 nm, respectively. As shown in Figs. 3(a) and 3(b), the reflectivity peak positions of the five grating periods are all at 1064 nm with almost no wavelength shift. (We select two methods of controlling variables.) The FWHM of the reflectivity curve decreases from 1.3 nm to 0.4 nm with the grating period increasing from 3450 nm to 11912 nm, as depicted in Fig. 3(c). (The FWHM is inversely proportional to the grating period, though it is only accurate to 0.1 nm.) Since the FWHM change curves obtained by these two methods of controlling variables are completely the same, the slot width does not affect the FWHM. Based on the above analysis, it can be concluded that the grating period mainly affects the location of the peak reflectivity and the FWHM of the reflectivity curve.

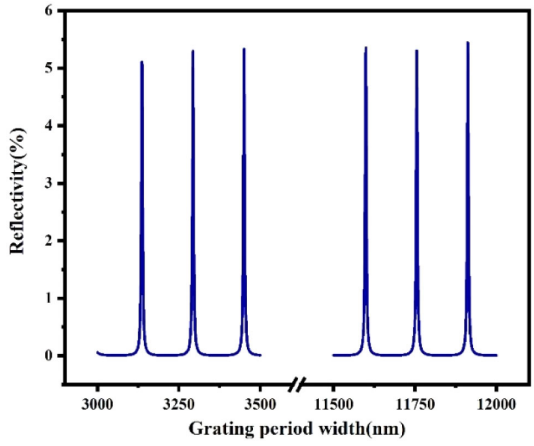

Fig. 2. Relation between grating period and grating reflectivity at a wavelength of 1064 nm.

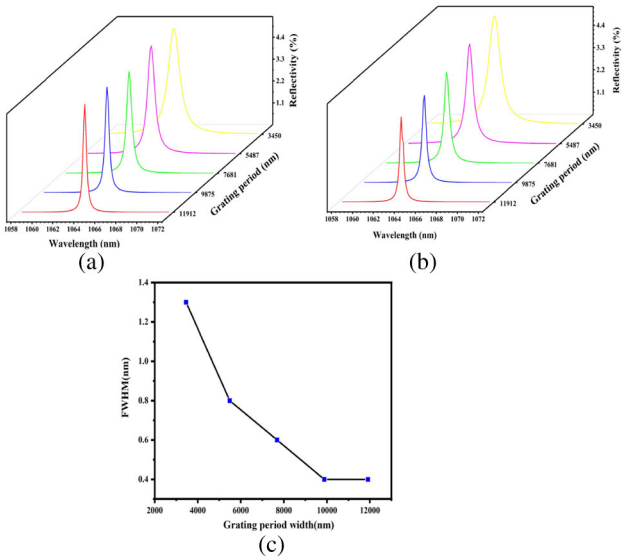

Fig. 3. (a) Relation between grating period and grating reflectivity (keeping the slot width at 1500 nm unchanged). (b) Relation between grating period and grating reflectivity (keeping the duty cycle at about 0.5 unchanged). (c) Variation of the FWHM with grating period.

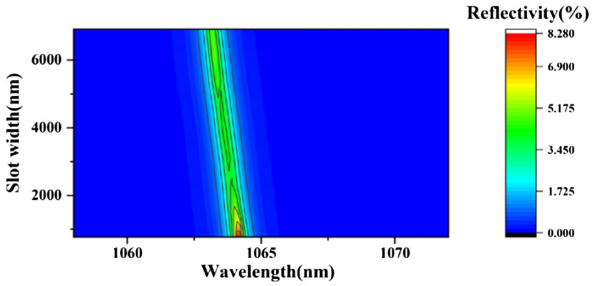

Fig. 4. Relation between slot width and grating reflectivity.

The effect of the slot width d_s on the spectral features was studied next. The grating period d_Λ and the etching depth h_{etch} are fixed to 7681 nm (corresponding to the highest reflectivity) and 1650 nm, respectively. The number of gratings N is set to 200. The wavelength range is set to 1058 nm to 1072 nm, and the interval is 0.1 nm. As shown in Fig. 4, the reflectivity of the grating becomes higher and the reflection peak slightly red shifted with increasing d_s. The FWHM of the reflectivity curve is almost unchanged. The main inference that can be drawn is that the slot width mainly affects the maximum reflectivity and slightly affects the location of the peak reflectivity. By calculating and observing Fig. 4, the FWHM does not change with the change of the slot width.

The variation reflectivity and loss of the gratings versus the etching depth h_{etch} and wavelength are shown in Fig. 5. The grating period d_Λ and the slot width d_s are fixed to 7681 nm and 1500 nm, respectively. The number of gratings N is still set to 200. Three periodic reflectivity peaks and the corresponding three periodic loss valleys appear in Figs. 5(a) and 5(b), respectively. The period between the two adjacent peaks (valleys) is about 21 nm. The reflectivity of the gratings increases and the loss decreases with the etching depth becoming deeper.

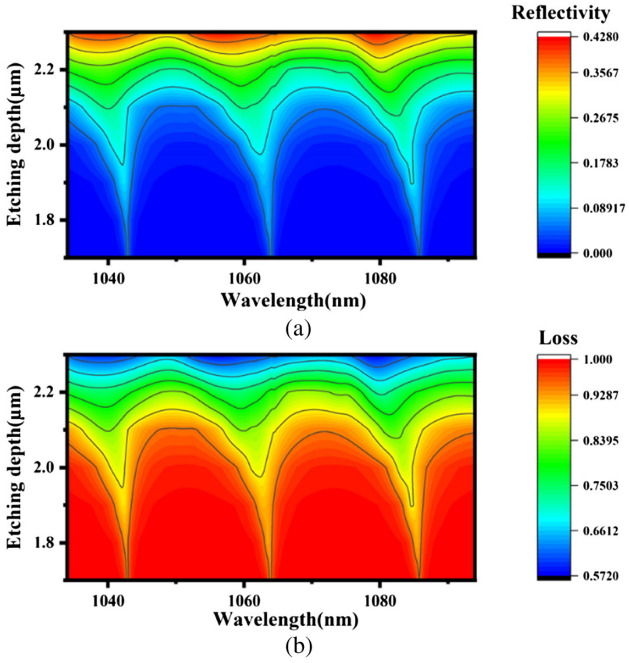

Fig. 5. (a) Relation between etching depth and grating reflectivity. (b) Relation between etching depth and grating loss.

While overly deep etching is bad for the performance of the gratings, the FWHM of the reflectivity curve increases rapidly with the etching depth becoming deeper. As shown in Fig. 5(a), the FWHM of the reflection curve reaches to 21 nm when etching depth h_{etch} is 2200 nm, which results in the gratings not being able to select the mode [21]. In order for the laser to select a single mode, the appropriate FWHM of the reflectivity curve should be 2–3 nm. The corresponding etching depth is 1900 nm, as shown in Fig. 5(a).

To make the most of the light, the number of gratings is set to 200 in the above analysis. In practice, the number of gratings required for high-order DBR semiconductor lasers is much less than 200. The variation of reflectivity versus the number of gratings N at different etching depths is shown in Fig. 6.

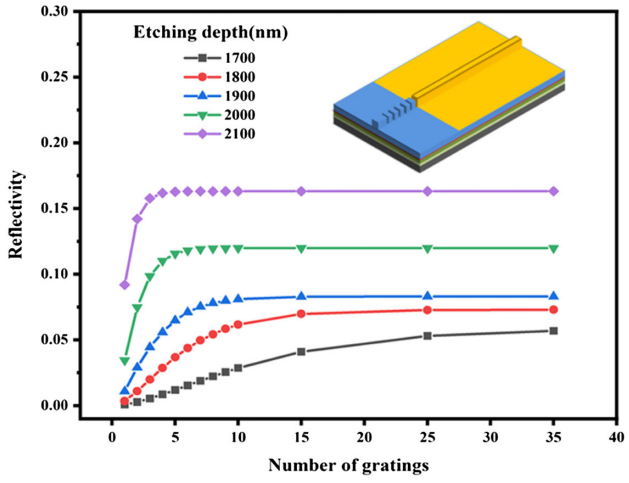

Fig. 6. Relation between the number of gratings and grating reflectivity; the three-dimensional schematic diagram of the epitaxial structure shows the position of the grating.

The grating period d_Λ and the slot width d_s are fixed to 7681 nm and 1500 nm, respectively. It can be seen from Fig. 6 that when the number of gratings reaches a certain number, the reflectivity maximizes and stays the same. The deeper the etching depth, the smaller the number of gratings needed to reach the maximum reflectivity [22]. According to the previous analysis, 15 pairs of gratings are appropriate to reach the maximum reflectivity when the etching depth is 1900 nm.

4. CONCLUSION

In this paper, the effects of different grating parameters on the spectra characteristics are investigated. The grating period mainly affects the location of peak reflectivity and the FWHM of the reflectivity curve but has almost no effect on the maximum reflectivity. The slot width mainly affects the maximum reflectivity and slightly affects the location of peak reflectivity, but it has almost no effect on the FWHM. The maximum reflectivity and the FWHM of the reflectivity curve become deeper as the etching depth increases. The reflectivity increases to the maximum and stays the same as the number of gratings increases. Based on the above conclusions, a set of grating parameters including a grating period of 7681 nm, slot width of 1500 nm, etching depth of 1900 nm, and grating number of 15 is optimal for a sufficiently high grating reflectivity of 6% and appropriate FWHM of 3 nm. This high-order Bragg grating structure with excellent performance can theoretically be used as a component of a narrow-linewidth DBR semiconductor laser.

Funding. National Key Research and Development Program of China (2018YFB2002400); National Natural Science Foundation of China (NSFC) (11674314, 11774343, 51672264, 61727822, 61804151, 61874117, 61874119); Jinan Science and Technology Plan (2019GXRC041); Science and Technology Development Project of Jilin Province (20180201014GX, 20180201119GX, 20200401006GX).

Disclosures. The authors declare no conflicts of interest.

REFERENCES

1. Z. Sodnik, B. Furch, and H. Lutz, "Optical intersatellite communication," IEEE J. Sel. Top. Quantum Electron. **16**, 1051–1057 (2010).
2. M. Takamoto, F. L. Hong, R. Higashi, and H. Katori, "An optical lattice clock," Nature **435**, 321–324 (2005).
3. S. Zlatanovic, J. S. Park, S. Moro, J. M. C. Boggio, I. B. Divliansky, N. Alic, S. Mookherjea, and S. Radic, "Mid-infrared wavelength conversion in silicon waveguides using ultracompact telecom-band-derived pump source," Nat. Photonics **4**, 561–564 (2010).
4. Y. Zhao, Y. Li, Q. Wang, F. Meng, Y. G. Lin, S. K. Wang, B. K. Lin, S. Y. Cao, J. P. Cao, Z. J. Fang, T. C. Li, and E. J. Zang, "100-Hz linewidth diode laser with external optical feedback," IEEE Photon. Technol. Lett. **24**, 1795–1798 (2012).
5. D. K. Shin, B. M. Henson, R. I. Khakimov, J. A. Ross, C. J. Dedman, S. S. Hodgman, K. G. H. Baldwin, and A. G. Truscott, "Widely tunable, narrow linewidth external-cavity gain chip laser for spectroscopy between 1.0–1.1 μm," Opt. Express **24**, 27403–27414 (2016).
6. B. Mroziewicz, "External cavity wavelength tunable semiconductor lasers—a review," Opto-Electron. Rev. **16**, 347–366 (2008).
7. I. Bayrakli, "Frequency stabilization at the sub-kilohertz level of an external cavity diode laser," Appl. Opt. **55**, 2463–2466 (2016).
8. I. Bayrakli, "Investigation of double-mode operation and fast fine tuning properties of a grating-coupled external cavity diode laser configuration," Opt. Laser Technol. **87**, 7–10 (2017).
9. M. Faugeron, M. Tran, O. Parillaud, M. Chtioui, Y. Robert, E. Vinet, A. Enard, J. Jacquet, and F. Van Dijk, "High-power tunable dilute mode DFB laser with low RIN and narrow linewidth," IEEE Photon. Technol. Lett. **25**, 7–10 (2013).
10. S. Spiessberger, M. Schiemangk, A. Wicht, H. Wenzel, O. Brox, and G. Erbert, "Narrow linewidth DFB lasers emitting near a wavelength of 1064 nm," J. Lightwave Technol. **28**, 2611–2616 (2010).
11. A. Klehr, S. Schwertfeger, H. Wenzel, T. Hoffmann, A. Liero, R. Staske, O. Brox, G. Erbert, and G. Trakle, "Dynamics of high power gain switched DFB RW laser under high current pulse excitation on a nanosecond time scale," Proc. SPIE **8640**, 86401N (2013).
12. P. Ma, A. Liu, F. Dong, M. Wang, and W. Zheng, "Single-mode semiconductor lasers fabricated by standard photolithography for direct modulation," Opt. Express **27**, 5502–5511 (2019).
13. J. J. Coleman, N. L. Dias, and U. Reddy, "Narrow spectral linewidth surface grating DBR diode lasers," in *23rd IEEE International Semiconductor Laser Conference* (IEEE, 2012), pp. 173–174.
14. S. Spiessberger, M. Schiemangk, A. Wicht, H. Wenzel, G. Erbert, and G. Trankle, "DBR laser diodes emitting near 1064 nm with a narrow intrinsic linewidth of 2 kHz," Appl. Phys. B **104**, 813–818 (2011).
15. J. Decker, P. Crump, J. Fricke, A. Maassdorf, G. Erbert, and G. Trankle, "Narrow stripe broad area lasers with high order distributed feedback surface gratings," IEEE Photon. Technol. Lett. **26**, 829–832 (2014).
16. F. G. Bachmann, "High-power diode laser technology and applications," Proc. SPIE **3888**, 394–403 (2000).
17. S. O'Brien and E. P. O'Reilly, "Theory of improved spectral purity in index patterned Fabry-Perot lasers," Appl. Phys. Lett. **86**, 201101 (2005).
18. Q. Y. Lu, W. H. Guo, R. Phelan, D. Byrne, J. F. Donegan, P. Lambkin, and B. Corbett, "Analysis of slot characteristics in slotted single-mode semiconductor lasers using the 2-D scattering matrix method," IEEE Photon. Technol. Lett. **18**, 2605–2607 (2006).
19. H. Wenzel, R. Guther, A. M. Shams-Zadeh-Amiri, and P. Bienstman, "A comparative study of higher order Bragg gratings: coupled-mode theory versus mode expansion modeling," IEEE J. Quantum Electron. **42**, 64–70 (2006).
20. W. Sun, Q. Lu, W. Guo, M. Wallace, F. Bello, and J. F. Donegan, "Analysis of high-order slotted surface gratings by the 2-D finite-difference time-domain method," J. Lightwave Technol. **35**, 96–102 (2017).
21. Q. Lu, W. Guo, D. Byrne, and J. F. Donegan, "Design of slotted single-mode lasers suitable for photonic integration," IEEE Photon. Technol. Lett. **22**, 787–789 (2010).
22. J. Fricke, F. Bugge, A. Ginolas, W. John, A. Klehr, M. Matalla, P. Ressel, H. Wenzel, and G. Erbert, "High-power 980-nm broad-area lasers spectrally stabilized by surface Bragg gratings," IEEE Photon. Technol. Lett. **22**, 284–286 (2010).